MAGNETOELASTIC ACTUATED MOTION OF FINE FERROMAGNETIC PARTICLES

GIOVANNI DI FRATTA, CLAUDIO SERPICO, AND VALERIY SLASTIKOV

Abstract. Wireless magnetic actuation offers precise control over microscopic devices, yet full planar manipulation of rigid, tethered magnetic particles remains challenging. We introduce a minimal variational model: a permanently magnetized planar ellipse anchored by two linear springs. First, we derive exact geometric conditions under which the springs can be configured so that the ellipse rotates freely without elastic penalty—producing a continuous family of zero-energy equilibria in which the ellipse's center traces a closed loop dictated solely by spring geometry. Next, we incorporate a uniform in-plane magnetic field and prove that the equilibrium magnetization aligns uniformly with the field. In the so-called full-controllability regime—when the spring rest lengths are long enough—rotating the external field directly prescribes the ellipse's orientation: the particle follows its zero-energy trajectory to maintain magnetic alignment, achieving a global energy minimum. For shorter springs, zero-energy configurations exist over a restricted orientation range; outside this range, the ellipse is pinned at the origin. Our results yield exact criteria for planar control in this simplest magnetoelastic setting, offering clear guidelines for the design of microscale actuators and metamaterials.

1. Introduction

The remote actuation of soft devices without onboard power is crucial for advances in microrobotics, biomedical engineering, and adaptive materials. By embedding magnetic nanoparticles within elastic substrates, one can induce rapid deformations when exposed to external magnetic fields. As a result, magnetic actuation strategies have become widespread in applications ranging from microelectromechanical systems (MEMS) and microfluidics to targeted biomedical interventions [14, 15, 19, 20].

A central concept in these systems is *magnetoelastic coupling*, whereby mechanical deformations and magnetic responses influence one another, enabling both locomotion and sensing at small scales. In soft composites with ferromagnetic inclusions, externally applied fields can induce bending, buckling, and twisting. These magnetoelastic systems have been investigated primarily through continuum approximations and molecular dynamics (MD) simulations, predicting a variety of instabilities, including buckling, dilation, and torsion [1, 2, 4, 16]. While these methods clarify many key mechanisms, their reliance on detailed simulations and approximate models often obscures the broader energy landscape and makes it difficult to extract simple, widely applicable design principles.

Here, we investigate a minimal magnetoelastic system: a uniformly magnetized rigid ellipse tethered by linear springs to a fixed frame, subject to a homogeneous in-plane magnetic field. Specifically, the ellipse (semi-major axis a) is attached to two linear springs of rest length L_0 and initial length L anchored at fixed points (cf. Figure 1). A

uniform, in-plane external field $\boldsymbol{h}_a$ of fixed magnitude but variable direction ψ serves as the sole control input. As ψ varies, one seeks to guide the ellipse's center $\boldsymbol{c} = (x, y) \in \mathbb{R}^2$ along a continuous closed trajectory while simultaneously adjusting its orientation θ. Remarkably, when $L_0 \geqslant L + 2a$, the system enters a *full-controllability regime*, allowing arbitrary planar positioning and rotation using only the single parameter ψ. Our analysis goes beyond small-deflection, linearized treatments by exploring the full nonlinear energy landscape associated with large deformations and rotations of the tethered ellipse.

The present minimal magnetoelastic system is the simplest analogue of a magnetically actuated element in soft matter. It models a rigid magnetic inclusion whose magnetic torque competes with an elastic restoring potential. Such idealized geometries — rods, ellipsoids, or disks embedded in or connected by elastic ligaments — occur across experimental platforms and length scales. For example, micrometer-scale ferromagnetic particles dispersed in soft polymer films and laminates form deformable composites that can display magnetoelastic instabilities and switchable bifurcations under applied fields [11, 16]. Magnetically driven MEMS commonly use rigid magnetic layers bonded to elastic substrates for microswitches, microinductors, and related devices [15]. Magnetic micro- and nanorobots often embed rigid magnetic elements in soft or biohybrid matrices to enable wireless, fuel-free propulsion and manipulation at low Reynolds numbers [10, 14, 19, 20]. Magnetoelastic metamaterials provide another pertinent example: their unit cells couple magnetic inclusions to elastic supports to produce strong, field-tunable mechanical and electromagnetic responses [13]. Recent experimental and theoretical studies of magnetoelastic membranes and paramagnetic filaments further reveal instability-driven actuation and collective dynamics under precessing or time-varying fields [1, 2, 4].

Within this experimental landscape, our minimal model isolates the core magnetoelastic competition by representing magnetic torques, dipolar interactions, and elastic restoring forces in a tractable framework. Despite its simplicity, it reproduces key scaling laws and qualitative behaviors seen in more complex systems — such as actuation thresholds, bistability, and orientational dynamics — and thus provides clear design principles for controllability and response in systems where magnetic torques and elastic restoring forces jointly determine deformation and orientation.

Outline. The remainder of the paper is organized as follows. In Section 2 we introduce our minimal elastic model of a rigid, permanently magnetized ellipse tethered by two linear springs and derive an explicit expression for its elastic energy (12). Section 3 is devoted to the purely elastic problem: we characterize all zero-energy configurations and prove Theorem 1. In Section 4 we couple the elastic model to a uniform in-plane magnetic field, show that the magnetization remains spatially uniform at equilibrium, and—under the same rest-length hypothesis—demonstrate full planar controllability by rotating the external field (Theorem 2). We also analyze the non-full-controllability regime $L < L_0 < L + 2a$, identifying when the ellipse must "pin" at the origin versus when it can still follow a zero-energy path.

2. The elastic model

What we are going to derive works for general bounded domains in $\mathbb{R}^2$. However, for concreteness, we assume that Ω is an ellipse in $\mathbb{R}^2$ made of ferromagnetic material. We assume (cf. Figure 1) that in the reference configuration Ω is centered at the origin, and its major axis is aligned along the $\boldsymbol{e}_1$ axis. We denote by $a > 0$ the length of its semi-major axis. The ellipse is elastically connected to two perpendicular walls at $\boldsymbol{w}_1 := -(a+L)\boldsymbol{e}_1$ and $\boldsymbol{w}_2 := (a + L)\boldsymbol{e}_1$ through linear springs, which are free to rotate about their pins. The springs are assumed to be at rest when their length is L_0. Hence, depending on the position of the walls, the initial length of the springs can be in an extension (if $L > L_0$) or compression (if $L < L_0$) state.

Assumption. *In this work, we assume that the initial (reference) length of the springs is in a compression state:*

$$L < L_0. \tag{1}$$

The regime $L \geqslant L_0$ can be investigated as well, but it is degenerate for our purposes as the critical points of $\mathcal{E}$ are isolated.

The state-space of Ω can be parameterized by the parameters $\boldsymbol{c} \in \mathbb{R}^2$ and $\theta \in \mathbb{R}$, which identify the center of the new position of Ω and the angle θ between its semi-major axis (initially in $\boldsymbol{e}_1$) and $\boldsymbol{e}_1$. We denote by $\Omega_{\boldsymbol{c},\theta}$ the state in which Ω is centered at $\boldsymbol{c} \in \mathbb{R}^2$ and rotated by an angle θ. Also, we denote by ℓ_1, ℓ_2 the increments of the springs connected, respectively, to $\boldsymbol{w}_1$ and $\boldsymbol{w}_2$, when the magnetic ellipse occupies the region $\Omega_{\boldsymbol{c},\theta}$. After nondimensionalization, the total elastic energy associated with the configuration $\Omega_{\boldsymbol{c},\theta}$ reads as

$$\mathcal{E}(\boldsymbol{c}, \theta) := \frac{1}{2}[(L - L_0) + \ell_1]^2 + \frac{1}{2}[(L - L_0) + \ell_2]^2. \tag{2}$$

To explicitly express the elastic energy $\mathcal{E}$ in terms of the state variables $\boldsymbol{c}, \theta$, we first observe (cf. Figure 1) that in terms of position vectors, the increments $L + \ell_i$ satisfy the relations

$$|L + \ell_1| = |\boldsymbol{\sigma}_1 - \boldsymbol{w}_1|, \tag{3}$$

$$|L + \ell_2| = |\boldsymbol{\sigma}_2 - \boldsymbol{w}_2|, \tag{4}$$

where $\boldsymbol{\sigma}_1, \boldsymbol{\sigma}_2$ are the position vectors of the extremities of the spring attached to $\Omega_{\boldsymbol{c},\theta}$ with respect to the origin. Simple vector algebra (cf. Figure 1) gives $\boldsymbol{\sigma}_1 = \boldsymbol{c} - aR_\theta\boldsymbol{e}_1$ and $\boldsymbol{\sigma}_2 = \boldsymbol{c} + aR_\theta\boldsymbol{e}_1$. Here, R_θ denotes the $2d$ rotation matrix

$$R_\theta := \begin{pmatrix} \cos\theta & -\sin\theta \\ \sin\theta & \cos\theta \end{pmatrix}. \tag{5}$$

Expanding the previous equations, we get

$$|L_0 + (L - L_0) + \ell_1| = |(a+L)\boldsymbol{e}_1 + (\boldsymbol{c} - aR_\theta\boldsymbol{e}_1)|, \tag{6}$$

$$|L_0 + (L - L_0) + \ell_2| = |(a+L)\boldsymbol{e}_1 - (\boldsymbol{c} + aR_\theta\boldsymbol{e}_1)|. \tag{7}$$

To further simplify the expressions (6) and (7), we rely on a classical physical assumption: the impenetrability of matter.
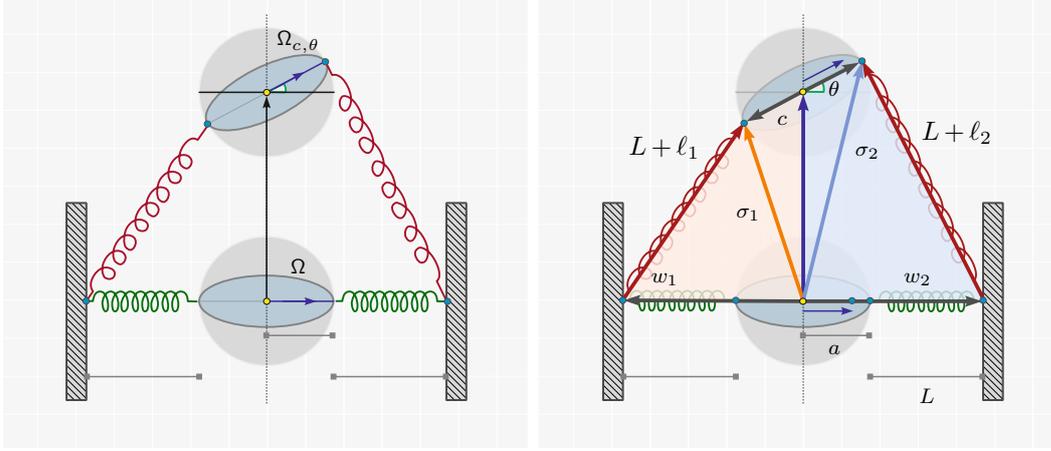
Figure 1. We assume that in the reference configuration Ω is centered at the origin and that its major axis is aligned along the e_1 axis. We denote by $a > 0$ the length of its semi-major axis. The ellipse is elastically connected to two perpendicular walls at $w_1 := -(a + L)e_1$ and $w_2 := (a + L)e_1$ through linear springs that are free to rotate about their pins. The springs are assumed to be at rest when their length is L_0. The state-space of Ω can be parameterized by the parameters $c \in \mathbb{R}^2$ and $\theta \in \mathbb{R}$ which identify the center of the new position of Ω and the angle θ between its semi-major axis (initially in e_1) and e_1.

Assumption. *We assume the impenetrability of matter, i.e., that the compression cannot collapse the spring to more than a single point. This amounts to requiring that $L + \ell_i \geqslant 0$ for $i = 1, 2$. Equivalently, we require that*

$$|\boldsymbol{\sigma}_i - \boldsymbol{w}_i| = L + \ell_i \quad (i = 1, 2). \tag{8}$$

Under assumption (8), the previous relations (6) and (7) can be rearranged under the form

$$(L - L_0) + \ell_1 = |(a + L)\boldsymbol{e}_1 + (\boldsymbol{c} - aR_\theta\boldsymbol{e}_1)| - L_0, \tag{9}$$

$$(L - L_0) + \ell_2 = |(a + L)\boldsymbol{e}_1 - (\boldsymbol{c} + aR_\theta\boldsymbol{e}_1)| - L_0. \tag{10}$$

Plugging the previous two relations into (2), we infer that in terms of the state variables $\boldsymbol{c}, \theta$, the total elastic energy reads as

$$\mathcal{E}(\boldsymbol{c}, \theta) = \frac{1}{2}\left(|(a + L)e_1 + (\boldsymbol{c} - aR_\theta\boldsymbol{e}_1)| - L_0\right)^2$$
$$+ \frac{1}{2}\left(|(a + L)\boldsymbol{e}_1 - (\boldsymbol{c} + aR_\theta\boldsymbol{e}_1)| - L_0\right)^2. \tag{11}$$

To shorten notation, we set

$$\mathcal{E}(\boldsymbol{c}, \theta) := \frac{1}{2}\left(|\boldsymbol{c} - \boldsymbol{v}_{a,L}(\theta)| - L_0\right)^2 + \frac{1}{2}\left(|\boldsymbol{c} + \boldsymbol{v}_{a,L}(\theta)| - L_0\right)^2, \tag{12}$$

with

$$\boldsymbol{v}_{a,L}(\theta) = aR_\theta\boldsymbol{e}_1 - (a + L)\boldsymbol{e}_1 = a\begin{pmatrix} \cos\theta - (1 + L/a) \\ \sin\theta \end{pmatrix}. \tag{13}$$

Remark 2.1. It is useful to keep in mind the geometric meaning of the vectors $c \pm v_{a,L}(\theta)$. They describe the segments occupied by the springs

$$c - v_{a,L}(\theta) = \sigma_1 - w_1, \tag{14}$$

$$c + v_{a,L}(\theta) = \sigma_2 - w_2. \tag{15}$$

For future reference, it is important to observe the estimates

$$|v_{a,L}(\theta)|^2 = a^2 \sin^2 \theta + (a(1 - \cos \theta) + L)^2 \geqslant L^2 \tag{16}$$

and

$$|v_{a,L}(\theta)|^2 \leqslant a^2 + (a + L)^2 \leqslant 2(a + L)^2, \tag{17}$$

which hold uniformly with respect to $\theta \in \mathbb{R}$.

Remark 2.2 (Modelling assumptions). For clarity, we summarize here the two modelling assumptions used throughout the paper. (i) The springs are attached to the frame by ideal hinges and are free to rotate at their ends; no bending moment is transmitted at the spring pins. (ii) Each spring is modeled as a linear axial spring (Hookean) that stores only stretch/compression energy and does not carry bending energy; consequently, Euler buckling of the springs is not included in the model. We also impose the impenetrability condition $L + \ell_i \geqslant 0$ (see (8)), which excludes spring collapse. Buckling and bending effects would require including spring bending stiffness and a stability analysis, and are therefore left to future work

3. MINIMIZERS OF THE ELASTIC ENERGY

In this section, we characterize the energy landscape described by the minimizers of the elastic energy (11). As we are going to show, the set of minimizers of $\mathcal{E}$ is degenerate in the sense that it is the image of a curve in $\mathbb{R}^2$.

Theorem 1. *Let*

$$\delta := \frac{L_0^2 - L^2}{2 a (a + L)},$$

and define the angular interval

$$I_\delta := \begin{cases} [-\cos^{-1}(1 - \delta), \cos^{-1}(1 - \delta)], & \text{if } L \leqslant L_0 \leqslant L + 2a, \\ [-\pi, \pi], & \text{if } L_0 \geqslant L + 2a. \end{cases} \tag{18}$$

Then the minimal value of the elastic energy $\mathcal{E}$ is zero. Moreover, this minimum is achieved if, and only if, (c, θ) belongs to the set $M \subseteq \mathbb{R}^2 \times [-\pi, \pi]$ generated by the graph of the closed curve

$$\gamma_\delta : \theta \in I_\delta \mapsto (c_1(\theta), c_2(\theta)) \in \mathbb{R}^2 \tag{19}$$

with

$$c_1(\theta) := \frac{c_2(\theta) \sin \theta}{(1 + L/a) - \cos \theta}, \tag{20}$$

$$c_2(\theta) := \left[\frac{(a(1 - \cos \theta) + L)^2 (L_0^2 - [L^2 + 2a(a + L)(1 - \cos \theta)])}{L^2 + 2a(a + L)(1 - \cos \theta)} \right]^{1/2}. \tag{21}$$
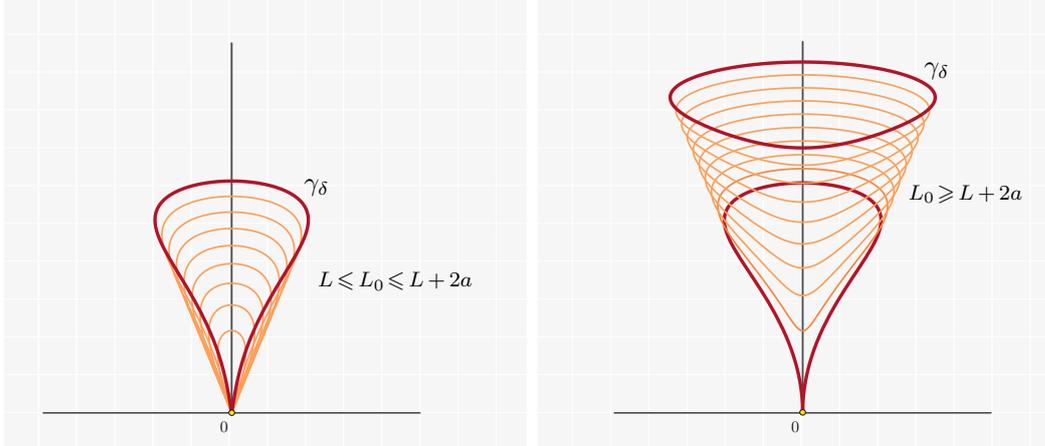
Figure 2. A qualitative plot of the family of trajectories that can be traced by the center c (without losing minimal elastic energy) for different values of $L_0 \geqslant L$. On the left part of the picture, we plot the regime $L \leqslant L_0 \leqslant L + 2a$, and on the right part of the picture, we plot the regime $L_0 \geqslant L + 2a$. Note that the curve γ_δ is a closed curve. Precisely, $\gamma_\delta(\pm \cos^{-1}(1 - \delta)) = (0, 0)$ if $L \leqslant L_0 \leqslant L + 2a$ and $\gamma_\delta(\pm\pi) = 0$ if $L_0 \geqslant L + 2a$. The maximum of $c_2(\theta)$ is reached at $\theta = 0$ where $c_2^2(0) = L_0^2 - L^2$. Instead, the minimum value of $c_2(\theta)$ depends on the regime. It is $c_2(\theta) = 0$ if $L \leqslant L_0 \leqslant L + 2a$, and $c_2^2(\theta) = L_0^2 - (2a + L)^2$ if $L_0 \geqslant L + 2a$.

Precisely, there holds

$$M := \{(\gamma_\delta(\theta), \theta) : \theta \in I_\delta\} \cup \{(-\gamma_\delta(\theta), \theta) : \theta \in I_\delta\}. \tag{22}$$

In particular, if $L_0 \geqslant L + 2a$, we have full controllability in the angle, that is, for every $\theta \in [-\pi, \pi]$ there exist centers $c := \pm\gamma_\delta(\theta)$ where the energy is minimized. Therefore, if $L_0 \geqslant L + 2a$, then Ω can be stabilized in any rotation state θ.

Before proving Theorem 1, we make some observations.

Remark 3.1. Note that γ_δ is a closed curve. Indeed, $\gamma_\delta(\pm \cos^{-1}(1 - \delta)) = (0, 0)$ if $L \leqslant L_0 \leqslant L + 2a$ and $\gamma_\delta(\pm\pi) = 0$ if $L_0 \geqslant L + 2a$. The maximum of $c_2(\theta)$ is always reached at $\theta = 0$ where $c_2^2(0) = L_0^2 - L^2$. Instead, the minimum value of $c_2(\theta)$ depends on the regime. It is $c_2(\theta) = 0$ (reached at $\theta = \pm \cos^{-1}(1 - \delta)$) if $L \leqslant L_0 \leqslant L + 2a$, and $c_2^2(\theta) = L_0^2 - (2a + L)^2$ (reached at $\theta = \pm\pi$) if $L_0 \geqslant L + 2a$. In Figure 2 we sketch, for different values of $L_0 \geqslant L$, a qualitative plot of the family of trajectories that can be traced by the center c (i.e., by the curve γ_δ) without altering the minimal elastic energy. On the left part of the picture, we plot the regime $L \leqslant L_0 \leqslant L + 2a$, and on the right part of the picture, we plot the regime $L_0 \geqslant L + 2a$.

Remark 3.2. It can be useful to know under which conditions the configurations $\Omega_{c, n\pi}$ ($n \in \mathbb{N}$) are energy minimizing. For that, note that If $\cos \theta = 1$, i.e., if $\theta = n\pi$, $n \in \mathbb{Z}$ and n even, then from (21) we get $c_2^2 = L_0^2 - L^2$. Therefore, $\Omega_{c, 0}$ is a minimizing configuration
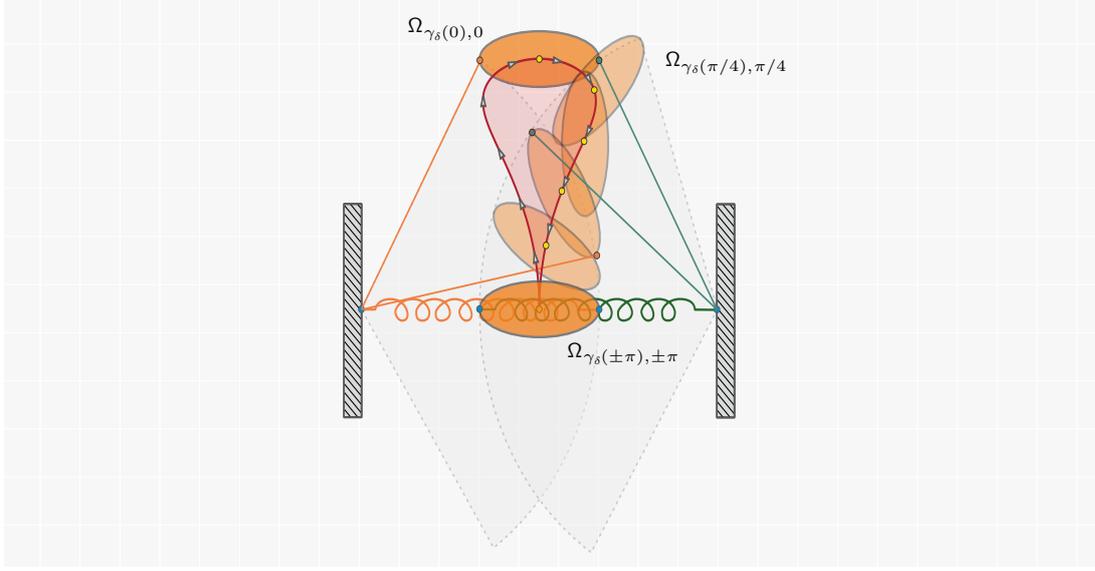
Figure 3. State-space of the system in the limiting case $L_0 = L + 2a$. The red curve represents $\gamma_\delta(\theta)$ which starts at $\theta = -\pi$ and ends at $\theta = \pi$. Note that for $\theta = \pm\pi$, the springs are attached to opposite vertices with respect to the reference configuration (this is energy favorable when $L_0 \geqslant L + 2a$).

only when $L_0 \geqslant L$. The minimizing configurations are associated with the centers

$$c = \left(0, \pm\sqrt{L_0^2 - L^2}\right).$$

Similarly, if $\cos\theta = -1$, i.e., if $\theta = n\pi$, $n \in \mathbb{Z}$ and n odd, then from (21) we get $c_2^2 = L_0^2 - (2a + L)^2$. Therefore, $\Omega_{c,\pi}$ and $\Omega_{c,-\pi}$ are minimizing configurations only when $L_0 \geqslant 2a + L$. The minimizing configurations are associated with the centers

$$c = \left(0, \pm\sqrt{L_0^2 - (2a + L)^2}\right).$$

Remark 3.3. It is enlightening to consider a concrete example. For $L = 2a$ and $L_0 = 4a$ we are in the limiting case $L_0 = L + 2a$. For every $\theta \in [-\pi, \pi]$ the equations (20) and (21) reduces to

$$c_2^2(\theta) = 3a^2 \frac{(3 - \cos\theta)^2(1 + \cos\theta)}{(5 - 3\cos\theta)}, \tag{23}$$

$$c_1(\theta) = \frac{c_2 \sin\theta}{3 - \cos\theta}. \tag{24}$$

Given the symmetries of the elastic system (cf. (28)), without loss of generality, we can focus on the positive brunch for $c_2(\theta)$. Plotting the curve $\gamma_\delta(\theta)$ for $\theta \in [-\pi, \pi]$, we get the admissible positions of the center c that minimize the energy. A plot in this limiting case $L_0 = L + 2a$, together with its physical meaning is given in Figure 3.

Proof. (OF THEOREM 1) We split the proof into three steps. The first step concerns the energy level associated with ground states, the second step is about symmetries of the minimizers.

Step 1. Minimizers have null energy. First, we show that if $(\boldsymbol{c}, \theta)$ is a minimizer of $\mathcal{E}$, then $\mathcal{E}(\boldsymbol{c}, \theta) = 0$. For that, we note that $\boldsymbol{v}_{a,L}(0) = -L\boldsymbol{e}_1$. Hence, for $\theta = 0$ and $\boldsymbol{c} = c_2\boldsymbol{e}_2$ the energy reduces to

$$\mathcal{E}\left(\boldsymbol{c}, 0\right) = \left(\sqrt{L^2 + c_2^2} - L_0\right)^2.$$

Taking $c_2^2 = L_0^2 - L^2 > 0$ (cf. (1)) we get

$$\mathcal{E}\left(\boldsymbol{c}, 0\right) = \left(\sqrt{L^2 + c_2^2} - L_0\right)^2 = 0.$$

Therefore, if $(\boldsymbol{c}, \theta)$ is a minimizer of $\mathcal{E}$ then

$$\left(|\boldsymbol{c} - \boldsymbol{v}_{a,L}(\theta)| - L_0\right)^2 = \left(|\boldsymbol{c} + \boldsymbol{v}_{a,L}(\theta)| - L_0\right)^2 = 0. \tag{25}$$

Step 2. Symmetries of the minimizers. We now show that if $(\boldsymbol{c}, \theta)$ is a minimizer of $\mathcal{E}$, so are

$$(-\boldsymbol{c}, \theta) = ((-c_1, -c_2), \theta), \tag{26}$$
$$(Z_{\pi/2}\boldsymbol{c}, -\theta) = ((-c_1, c_2), -\theta), \tag{27}$$
$$(Z_\pi\boldsymbol{c}, -\theta) = ((c_1, -c_2), -\theta). \tag{28}$$

First, the invariance of the Euclidean norm under rotations gives $\mathcal{E}\left(-\boldsymbol{c}, \theta\right) = \mathcal{E}\left(\boldsymbol{c}, \theta\right)$. Also, if we denote by Z_ϕ the reflection about a line through the origin that makes an angle ϕ with the x-axis, i.e.,

$$Z_\phi := \left(\begin{array}{cc} \cos 2\theta & \sin 2\theta \\ \sin 2\theta & -\cos 2\theta \end{array}\right)$$

then

$$Z_\phi \boldsymbol{v}_{a,L}(\theta) = a\left(\begin{array}{c} \cos(\theta - 2\phi) - (1 + L/a)\cos 2\phi \\ -\sin(\theta - 2\phi) - (1 + L/a)\sin 2\phi \end{array}\right).$$

We deduce that $Z_\phi \boldsymbol{v}_{a,L}(\theta) = -\boldsymbol{v}_{a,L}(-\theta)$ when $\phi = +\pi/2$ (reflection about the y axis). Moreover, we have that $Z_\phi \boldsymbol{v}_{a,L}(\theta) = \boldsymbol{v}_{a,L}(-\theta)$ when $\phi = \pi$ (reflection about the x axis).

Step 3. Characterization of the minimizers. By (25) we know that the minimal elastic energy is reached when the relations $|\boldsymbol{c} - \boldsymbol{v}_{a,L}(\theta)| = |\boldsymbol{c} + \boldsymbol{v}_{a,L}(\theta)| = L_0$ are satisfied. A direct computation shows that the equation $|\boldsymbol{c} - \boldsymbol{v}_{a,L}(\theta)|^2 = |\boldsymbol{c} + \boldsymbol{v}_{a,L}(\theta)|^2$ is satisfied when

$$c_1 := \frac{c_2 \sin \theta}{(1 + L/a) - \cos \theta}. \tag{29}$$

Note that the denominator is always strictly positive. Expanding the equation

$$|\boldsymbol{c} + \boldsymbol{v}_{a,L}(\theta)|^2 = L_0^2 \tag{30}$$

and taking into account the expression of c_1 in (29), we get that

$$c_2^2 = \frac{(a(1 - \cos \theta) + L)^2(L_0^2 - [L^2 + 2a(a + L)(1 - \cos \theta)])}{L^2 + 2a(a + L)(1 - \cos \theta)}. \tag{31}$$

The existence of a solution is constrained to the condition that the right-hand side of (31) is nonnegative, i.e., provided that $L_0^2 \geqslant L^2 + 2a(a + L)(1 - \cos \theta)$. This is equivalent to

$$\cos \theta \geqslant \frac{L^2 + 2a(a + L) - L_0^2}{2a(a + L)} = 1 - \frac{L_0^2 - L^2}{2a(a + L)}. \tag{32}$$

Observe that the previous inequality in θ is well-posed due to the regime of compression we are investigating where $L_0 \geqslant L$. After that, any $\theta \in \mathbb{R}$ is a solution of (32) if

$$1 - \frac{L_0^2 - L^2}{2a(a+L)} \leqslant -1 \tag{33}$$

i.e., when $L_0 \geqslant L + 2a$. Instead, if $0 < L_0 < L + 2a$, then we have only a subset of angles that solves (32) and this is given by the interval where

$$|\theta| \leqslant \cos^{-1}(1 - \delta), \quad \delta := \frac{L_0^2 - L^2}{2a(a+L)} \tag{34}$$

Overall, it follows that for any given θ there exists *at most* a solution $(c_1(\theta), c_2(\theta))$, and this is given by (20) and (21). Moreover, from the symmetries of the elastic system (cf. (28)), we deduce that if $L_0 \geqslant L + 2a$, then for every θ there exists a unique $(c_1, c_2) \in \mathbb{R}^2, c_2 \geqslant 0$, such that $\Omega_{\boldsymbol{c},\theta}$ is at minimal energy with angle θ. In particular, we have full controllability in the angle θ when $L_0 \geqslant L + 2a$. Instead, if $L < L_0 < L + 2a$, then the minimizers of the elastic energy are the image of the curve

$$\gamma_\delta(\theta) = (c_1(\theta), c_2(\theta)) \quad \text{with} \quad \theta \in I_\delta := [-\cos^{-1}(1 - \delta), \cos^{-1}(1 - \delta)].$$

In particular, for any $|\theta| \leqslant \cos^{-1}(1 - \delta)$ there exists a unique $\boldsymbol{c} \in \mathbb{R}^2, c_2 \geqslant 0$, such that $\Omega_{\boldsymbol{c},\theta}$ is at minimal energy with angle θ. Combining these observations with the symmetry properties of the elastic system (cf. (28)), we get the characterization of the energy landscape given in (22). □

4. MINIMIZERS OF THE MAGNETOELASTIC SYSTEM

Our investigation targets the *small-scale* regime, in which device dimensions become comparable to the magnetic exchange length. In this limit, the variational theory of micromagnetics offers a natural description: the magnetization is represented by a unit-length vector field that minimizes a total energy functional comprised of exchange, crystalline anisotropy, Zeeman, and demagnetizing terms [3, 7, 12]. Crucially, this variational setting is well-suited to include elastic effects by introducing a coupled energy that depends jointly on the strain field and the magnetization. In a two-dimensional formulation, and after nondimensionalization, the magnetic energy of an elastic ellipse $\Omega_{\boldsymbol{c},\theta}$ in the deformed state characterized by parameters $(\boldsymbol{c}, \theta)$ is expressed as follows [8, 11]:

$$\mathcal{F}_{\Omega_{\boldsymbol{c},\theta}}(\boldsymbol{m}; \theta) := \frac{1}{|\Omega_{\boldsymbol{c},\theta}|} \Big[\int_{\Omega_{\boldsymbol{c},\theta}} a_{\mathrm{ex}}^2 |\nabla \boldsymbol{m}|^2 + \kappa^2 \int_{\Omega_{\boldsymbol{c},\theta}} (\boldsymbol{m} \cdot \boldsymbol{e}_3)^2$$
$$- \int_{\Omega_{\boldsymbol{c},\theta}} \boldsymbol{h}_a \cdot \boldsymbol{m} + \frac{\kappa_{\mathrm{an}}^2}{2} \int_{\Omega_{\boldsymbol{c},\theta}} |\boldsymbol{m} \times \boldsymbol{e}_\theta|^2 \Big] \tag{35}$$

for $\boldsymbol{m} \in H^1(\Omega_{\boldsymbol{c},\theta}, \mathbb{S}^2)$. If Ω is the reference ellipse centered at the origin as in Figure 1, then $\Omega_{\boldsymbol{c},\theta}$ is the image under Ω of the map

$$\mu_{\boldsymbol{c},\theta} : x \in \Omega \mapsto (R_\theta x + \boldsymbol{c}) \in \Omega_{\boldsymbol{c},\theta}.$$

Here R_θ is the three-dimensional rotation matrix about the out-of-plane $\boldsymbol{e}_3$-axis. To simplify the exposition, we assume that in the reference configuration, the direction of the anisotropy axis corresponds to $\boldsymbol{e}_1$. Therefore $\boldsymbol{e}_\theta := R_\theta \boldsymbol{e}_1$. Note that, with a small abuse of

the notation, we denote by the same symbols the basis vectors in $\mathbb{R}^2$ and $\mathbb{R}^3$. The context clarifies what is meant.

The total magnetoelastic energy associated with the system in the configuration $\Omega_{c,\theta}$ reads as

$$\mathcal{G}\left(\boldsymbol{m};\boldsymbol{c},\theta\right) = \mathcal{E}(\boldsymbol{c},\theta) + \mathcal{F}_{\Omega_{c,\theta}}\left(\boldsymbol{m};\theta\right).$$

We are interested in the minimization problem

$$\min_{(\boldsymbol{c},\theta)\in\mathbb{R}^2\times[-\pi,\pi]}\left(\mathcal{E}(\boldsymbol{c},\theta) + \min_{\boldsymbol{m}\in H^1(\Omega_{c,\theta},\mathbb{S}^2)}\mathcal{F}_{\Omega_{c,\theta}}\left(\boldsymbol{m};\theta\right)\right). \tag{36}$$

Remark 4.1. For notational simplicity, we set the spring stiffness to unity in our nondimensional formulation. Introducing an explicit spring constant $k > 0$ only rescales the relative weight of elastic and magnetic energies. Concretely, if the elastic energy is written as

$$\mathcal{E}_k(\boldsymbol{c},\theta) = \frac{k}{2}((\mid \boldsymbol{c} - \boldsymbol{v}_{a,L}(\theta)\mid -L_0)^2 + (\mid \boldsymbol{c} + \boldsymbol{v}_{a,L}(\theta)\mid -L_0)^2),$$

then the total energy becomes $\mathcal{F} + \mathcal{E}_k$, which is variationally equivalent to $\mathcal{F}/k + \mathcal{E}$. Hence, one may introduce the effective magnetic parameters

$$|\boldsymbol{h}_a|_{\text{eff}} = \frac{|\boldsymbol{h}_a|}{k}, \quad \kappa_{\text{an,eff}} = \frac{\kappa_{\text{an}}}{\sqrt{k}}.$$

Accordingly, increasing the spring stiffness k decreases the effective applied field and anisotropy relative to elastic forces. Thus, varying k produces a quantitative rescaling of the parameter regime, but does not introduce qualitatively new behavior. For this reason, we set $k = 1$ throughout the paper.

Our main result reads as follows.

Theorem 2. *Let $\boldsymbol{h}_a \neq 0$ and $\psi \in [-\pi, \pi]$ the angle that the applied field $\boldsymbol{h}_a$ makes with $\boldsymbol{e}_1$. If $(\boldsymbol{m};\boldsymbol{c},\theta)$ in $H^1\left(\Omega_{c,\theta},\mathbb{S}^2\right) \times \mathbb{R}^2 \times [-\pi,\pi]$ is a minimizer of the energy functional $\mathcal{G}$ then $\boldsymbol{m} \in \mathbb{S}^1$, i.e., $\boldsymbol{m}$ is constant in $\Omega_{c,\theta}$.*

Moreover, if

$$\psi \in [-\cos^{-1}(1-\delta), \cos^{-1}(1-\delta)], \quad \delta := \frac{L_0^2 - L^2}{2a(a+L)}, \tag{37}$$

then the magnetoelastic minimizers are given by

$$\boldsymbol{m} = \boldsymbol{h}_a/|\boldsymbol{h}_a|, \quad \boldsymbol{e}_\theta = \pm\boldsymbol{h}_a/|\boldsymbol{h}_a|, \quad \boldsymbol{c} = \gamma_\delta(\theta),$$

with $\theta = \psi + k\pi$, $k \in \mathbb{Z}$, and $\boldsymbol{c} = \gamma_\delta(\theta)$ the curve characterized in Theorem 1. The minimal value of the energy is then $\mathcal{G}\left(\boldsymbol{m};\boldsymbol{c},\theta\right) = -|\boldsymbol{h}_a|$. In particular, in the full controllability regime $L_0 \geqslant L + 2a$, the characterization holds for every $\psi \in [-\pi,\pi]$.

Instead, if (37) does not hold, i.e., if $\psi \notin [-\cos^{-1}(1-\delta), \cos^{-1}(1-\delta)]$ and, therefore, necessarily $L < L_0 < L + 2a$, the following assertions hold. If $(\boldsymbol{m};\boldsymbol{c},\theta)$ is a minimizer of $\mathcal{G}$ the following dichotomy holds:

i. *Either $\cos\theta \geqslant 1-\delta$; in which case $\mathcal{E}(\boldsymbol{c},\theta) = 0$ with the optimal center $\boldsymbol{c}$ determined by the curve γ_δ defined by (20) and (21),*

ii.   or else, $\cos\theta < 1 - \delta$; in which case $\boldsymbol{c} = 0$.

Therefore, if $\cos\theta < 1 - \delta$ then any minimizer $(\boldsymbol{m}; \boldsymbol{c}, \theta)$ of $\mathcal{G}$ is centered at the origin, i.e., of the form $(\boldsymbol{m}; 0, \theta)$, with $(\boldsymbol{m}, \theta)$ minimizer in $\mathbb{S}^1 \times [-\pi, \pi]$ of the energy

$$\mathcal{F}(\boldsymbol{m}; \theta) := -\boldsymbol{h}_a \cdot \boldsymbol{m} + \frac{\kappa_{\mathrm{an}}^2}{2} |\boldsymbol{m} \times \boldsymbol{e}_\theta|^2 + (|\boldsymbol{v}_{a,L}(\theta)| - L_0)^2. \qquad (38)$$

Equivalently, if we express the quantities in polar coordinates through the angles (ϕ, ψ) such that $\boldsymbol{m} := R_\phi e_1$ and $\boldsymbol{h}_a := |\boldsymbol{h}_a| R_\psi e_1$, then (38) reads as

$$\mathcal{F}(\boldsymbol{m}; \theta) = \frac{\kappa_{\mathrm{an}}^2}{2} \sin^2(\theta - \phi) - |\boldsymbol{h}_a| \cos(\psi - \phi) + (|\boldsymbol{v}_{a,L}(\theta)| - L_0)^2. \qquad (39)$$

Remark 4.2. In the limiting case $L_0 = L$, the parameter δ in (37) vanishes. Consequently, when $\boldsymbol{h}_a$ is not aligned with $\boldsymbol{e}_1$, the minimization problem reduces to that of the energy functional (39). This functional is nonconvex and can be viewed as a natural generalization of the classical Stoner–Wohlfarth model [17]: the first two terms of (39) reproduce the Stoner–Wohlfarth energy, while the additional term represents the elastic coupling. A systematic analysis of the resulting energy landscape is of clear interest but lies outside the scope of the present work.

In Figure 4 we represent the magnetoelastic energy minimizers associated with a full rotation of the applied field $\boldsymbol{h}_a$ (encoded in the angle ψ) in the interval $[0, 2\pi]$. In order to catch the nonfull controllability regime $L < L_0 < L + 2a$, we set $L = 3a$ and $L_0 = L + a$. Also, we set $|\boldsymbol{h}_a| = 1$ and $\kappa_{\mathrm{an}} = 2$. This choice entails that the minimal magnetization $\boldsymbol{m}$ is not aligned with the applied field $\boldsymbol{h}_a$ when the associated angle ψ is such that $\cos\psi < 1 - \delta$ (see the configuration at $\boldsymbol{c} = 0$). Note that, without any loss of generality, in Figure 4, we can restrict the visualization to the case $c_2 \geqslant 0$. Indeed, we already pointed out that if $(\boldsymbol{c}, \theta)$ is a minimizer of the elastic energy $\mathcal{E}$, so are (cf. (28)) $(-\boldsymbol{c}, \theta)$, $(Z_{\pi/2}\boldsymbol{c}, -\theta)$, $(Z_\pi \boldsymbol{c}, -\theta)$. This is because of

$$\mathcal{E}(\boldsymbol{c}, \theta) = \mathcal{E}(-\boldsymbol{c}, \theta) = \mathcal{E}(Z_{\pi/2}\boldsymbol{c}, -\theta) = \mathcal{E}(Z_\pi \boldsymbol{c}, -\theta).$$

The previous relations imply similar symmetry relations on the magnetoelastic energy $\mathcal{F}$. Precisely, if we set

$$\mathcal{F}_\psi(\boldsymbol{m}; \boldsymbol{c}, \theta) = \frac{\kappa_{\mathrm{an}}^2}{2} \sin^2(\theta - \phi) - |\boldsymbol{h}_a| \cos(\psi - \phi) + \mathcal{E}(\boldsymbol{c}, \theta)$$

so that the notation for $\mathcal{F}$ also the dependence from the external field direction ψ, then we have

$$\mathcal{F}_\psi(\phi; \boldsymbol{c}, \theta) = \mathcal{F}_\psi(\phi; -\boldsymbol{c}, \theta) = \mathcal{F}_{-\psi}(-\phi, Z_{\pi/2}\boldsymbol{c}, -\theta) = \mathcal{F}_{-\psi}(-\phi, Z_\pi \boldsymbol{c}, -\theta).$$

Therefore, the visualization of the energy landscape for $c_2 \geqslant 0$ does not affect any generality.

Before the proof of Theorem 2 we make some observations and prove complementary results.

Remark 4.3. The analysis of the minimizers in the elastic regime is independent of the shape of Ω. Indeed, it depends only on the segment of length $2a$ passing through Ω to which the springs are connected.
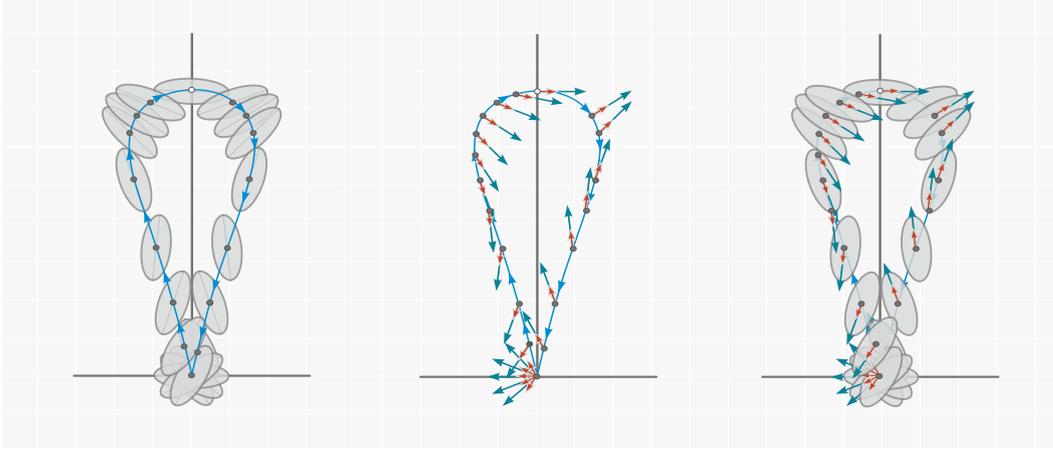
Figure 4. Numerical computation of the magnetoelastic energy landscape associated with a full rotation of the applied field $\boldsymbol{h}_a$ (encoded in the angle ψ) in the interval $[0, 2\pi]$. Here, we set $L = 3a$ and $L_0 = L + a$ so that we are in the nonfull controllability regime $L < L_0 < L + 2a$. Also, we set $|\boldsymbol{h}_a| = 1$ and $\kappa_{\mathrm{an}} = 2$. This choice entails that the minimal magnetization $\boldsymbol{m}$ (in red in the Figure) is not aligned with the applied field $\boldsymbol{h}_a$ (in cyan in the Figure) when the associated angle ψ is outside of the interval $[-\cos^{-1}(1-\delta), \cos^{-1}(1-\delta)]$ (see the configuration pinned at $\boldsymbol{c} = 0$). Left, position and orientation of the ellipse as ψ varies in the interval $[0, 2\pi]$. When $\psi = 0$, the center of the ellipse is on the y axis and is represented by a white dot. As ψ varies in $[0, 2\pi]$ the ellipse rotates and moves along the curve γ_δ (represented in light blue in the picture. Center, for clarity, we represent the minimal magnetization $\boldsymbol{m}$ (in dark red) associated with the applied field $\boldsymbol{h}_a$. Right, we overlap the two plots so as to have a complete picture of the induced dynamics.

Remark 4.4. Intuitively, the energy in (39) reveals that the higher is $|\boldsymbol{h}_a|$, the more the magnetization $\boldsymbol{m}$ (in terms of ϕ) tends to be aligned with the field $\boldsymbol{h}_a$. Also, the higher is κ_{an}^2, the more the axis of Ω (expressed in terms of θ) tends to follow the orientation of $\boldsymbol{m}$. To make these statements quantitative, we prove the following result.

Proposition 1. *If* $(\boldsymbol{m}; \boldsymbol{c}, \theta)$ *is a minimum point for* $\mathcal{F}$ *in* (39) *then*

$$|\sin(\phi - \psi)| \leqslant \frac{1}{2|\boldsymbol{h}_a|} \tag{40}$$

and

$$|\sin(2(\theta - \phi))| \leqslant \frac{1}{\kappa_{\mathrm{an}}^2}. \tag{41}$$

Remark 4.5. Relation (41) gives a quantitative justification to the observation that the bigger is κ_{an}^2, the more is $(\theta - \phi)$ close to the set $\{-\pi/2, 0, \pi/2, \pi\}$. Also, (40) tells us that the bigger is $|\boldsymbol{h}_a|$ the more is $(\phi - \psi)$ close to the set $\{0, \pi\}$. In terms of limiting relations, this tells us that

$$\sphericalangle(\boldsymbol{m} \cdot \boldsymbol{e}_\theta) \xrightarrow{\kappa_{\mathrm{an}} \to \infty} \{-\pi/2, 0, \pi/2, \pi\}, \quad \sphericalangle(\boldsymbol{m} \cdot \boldsymbol{h}_a) \xrightarrow{|\boldsymbol{h}_a| \to \infty} \{0, \pi\},$$

where $\boldsymbol{e}_\theta$ coincides with the axis of the ellipse to the extremities of which the springs are attached. On the other hand, by minimality, we know that if $(\boldsymbol{m}; \boldsymbol{c}, \theta)$ minimizes the energy, then necessarily $\sphericalangle(\boldsymbol{m} \cdot \boldsymbol{h}_a) \leqslant \pi/2$ because if $\sphericalangle(\boldsymbol{m} \cdot \boldsymbol{h}_a) > \pi/2$, one can

decrease the energy by reversing the magnetization from $\boldsymbol{m}$ to $-\boldsymbol{m}$. This is because the only part of the energy that depends on $\boldsymbol{m}$ is the density $-\boldsymbol{h}_a \cdot \boldsymbol{m} + \frac{\kappa_{\mathrm{an}}^2}{2} |\boldsymbol{m} \times \boldsymbol{e}_\theta|^2$ and, therefore, switching from $\boldsymbol{m}$ to $-\boldsymbol{m}$ does not alter the anisotropy energy while reducing the Zeeman energy. Overall, we get that

$$\sphericalangle(\boldsymbol{m} \cdot \boldsymbol{e}_\theta) \xrightarrow{\kappa_{\mathrm{an}} \to \infty} \{-\pi/2, 0, \pi/2, \pi\}, \quad \sphericalangle(\boldsymbol{m} \cdot \boldsymbol{h}_a) \xrightarrow{|\boldsymbol{h}_a| \to \infty} \{0\}.$$

Proof. (of Proposition 1) Let $(\boldsymbol{m}; \boldsymbol{c}, \theta)$ be a minimizer of $\mathcal{F}$ in (39). From the stationary condition $\partial_{\boldsymbol{m}} \mathcal{F}(\boldsymbol{m}; \boldsymbol{c}, \theta) = 0$ we get that the following Euler–Lagrange holds

$$(\boldsymbol{m} \cdot \boldsymbol{e}_\theta) \boldsymbol{e}_\theta + \boldsymbol{h}_a = \lambda \boldsymbol{m}, \qquad \lambda := (\boldsymbol{m} \cdot \boldsymbol{e}_\theta)^2 + \boldsymbol{m} \cdot \boldsymbol{h}_a, \tag{42}$$

with λ the Lagrange multiplier coming from the nonconvex constraint $\boldsymbol{m} \in \mathbb{S}^1$. By cross-multiplying both sides of the Euler–Lagrange equation by $\boldsymbol{e}_\theta$ we get $(\boldsymbol{h}_a \times \boldsymbol{e}_\theta) = \lambda(\boldsymbol{m} \times \boldsymbol{e}_\theta)$, from which

$$|\boldsymbol{h}_a|^2 - (\boldsymbol{e}_\theta \cdot \boldsymbol{h}_a)^2 = \left((\boldsymbol{m} \cdot \boldsymbol{e}_\theta)^2 + (\boldsymbol{m} \cdot \boldsymbol{h}_a)\right)^2 \left(1 - (\boldsymbol{m} \cdot \boldsymbol{e}_\theta)^2\right). \tag{43}$$

Dot multiplying both sides of the Euler–Lagrange equation by $\boldsymbol{e}_\theta$ we get $(\boldsymbol{m} \cdot \boldsymbol{e}_\theta) + (\boldsymbol{e}_\theta \cdot \boldsymbol{h}_a) = \lambda(\boldsymbol{m} \cdot \boldsymbol{e}_\theta)$, from which it follows that

$$(\boldsymbol{e}_\theta \cdot \boldsymbol{h}_a) = \left((\boldsymbol{m} \cdot \boldsymbol{e}_\theta)^2 + (\boldsymbol{m} \cdot \boldsymbol{h}_a) - 1\right)(\boldsymbol{m} \cdot \boldsymbol{e}_\theta). \tag{44}$$

Combining (43) and (44) through the in common term $(\boldsymbol{e}_\theta \cdot \boldsymbol{h}_a)$ we get the relation

$$|\boldsymbol{h}_a|^2 - \left((\boldsymbol{m} \cdot \boldsymbol{e}_\theta)^2 + (\boldsymbol{m} \cdot \boldsymbol{h}_a) - 1\right)^2 (\boldsymbol{m} \cdot \boldsymbol{e}_\theta)^2 = \left((\boldsymbol{m} \cdot \boldsymbol{e}_\theta)^2 + (\boldsymbol{m} \cdot \boldsymbol{h}_a)\right)^2 \left(1 - (\boldsymbol{m} \cdot \boldsymbol{e}_\theta)^2\right),$$

which, after some algebra, reduces to the equation

$$(\boldsymbol{m} \cdot \boldsymbol{e}_\theta)^4 - (\boldsymbol{m} \cdot \boldsymbol{e}_\theta)^2 + |\boldsymbol{h}_a \times \boldsymbol{m}|^2 = 0. \tag{45}$$

Therefore the solutions of (45) satisfy the relation

$$(\boldsymbol{m} \cdot \boldsymbol{e}_\theta)^2 = \frac{1 \pm \sqrt{1 - 4|\boldsymbol{h}_a \times \boldsymbol{m}|^2}}{2}. \tag{46}$$

Since we know about the existence of solutions, this implies that

$$\frac{1}{4} \geqslant |\boldsymbol{h}_a \times \boldsymbol{m}|^2. \tag{47}$$

In terms of angles, the previous relation reads as $|\sin(\phi - \psi)| \leqslant 1/2|\boldsymbol{h}_a|$, which is exactly (40). After that, if $(\boldsymbol{m}; \boldsymbol{c}, \theta)$ is a minimizer, then also the stationary condition $\partial_\phi \mathcal{F}(\boldsymbol{m}; \boldsymbol{c}, \theta) = 0$ holds. In polar coordinates, the stationary condition $\partial_\phi \mathcal{F}(\boldsymbol{m}; \boldsymbol{c}, \theta) = 0$ reads as

$$\frac{\kappa_{\mathrm{an}}^2}{2} \sin(2(\theta - \phi)) = |\boldsymbol{h}_a| \sin(\phi - \psi). \tag{48}$$

Combining (40) and (48) we get (41). □

Proof. (*of* Theorem 2) We divide the proof into three steps.

Step 1. Magnetoelastic minimizers have $\boldsymbol{m} \in \mathbb{S}^1$. Our first step shows that if $(\boldsymbol{m}; \boldsymbol{c}, \theta)$ is a minimizer in $H^1(\Omega_{\boldsymbol{c},\theta}, \mathbb{S}^2) \times \mathbb{R}^2 \times [-\pi, \pi]$ of the energy functional $\mathcal{G}$ then $\boldsymbol{m} \in \mathbb{S}^1$, i.e., $\boldsymbol{m}$ is constant in $\Omega_{\boldsymbol{c},\theta}$. Moreover, the minimization problem (36) is equivalent to

$$\min_{(\boldsymbol{c},\theta) \in \mathbb{R}^2 \times [-\pi,\pi]} \left(\min_{\boldsymbol{m} \in \mathbb{S}^1} \left[-\boldsymbol{h}_a \cdot \boldsymbol{m} + \frac{\kappa_{\mathrm{an}}^2}{2} |\boldsymbol{m} \times \boldsymbol{e}_\theta|^2 \right] + \mathcal{E}(\boldsymbol{c}, \theta) \right). \qquad (49)$$

Indeed, we have

$$\mathcal{G}(\boldsymbol{m}; \boldsymbol{c}, \theta) \geqslant \min_{(\boldsymbol{c},\theta) \in \mathbb{R}^2 \times [-\pi,\pi]} \left(\min_{\boldsymbol{m} \in \mathbb{S}^2} \left[\frac{\kappa^2}{2} (\boldsymbol{m} \cdot \boldsymbol{e}_3)^2 - \boldsymbol{h}_a \cdot \boldsymbol{m} + \frac{\kappa_{\mathrm{an}}^2}{2} |\boldsymbol{m} \times \boldsymbol{e}_\theta|^2 \right] + \mathcal{E}(\boldsymbol{c}, \theta) \right)$$

$$\geqslant \min_{(\boldsymbol{c},\theta) \in \mathbb{R}^2 \times [-\pi,\pi]} \left(\min_{\boldsymbol{m} \in \mathbb{S}^2} \left[-\boldsymbol{h}_a \cdot \boldsymbol{m} + \frac{\kappa_{\mathrm{an}}^2}{2} |\boldsymbol{m} \times \boldsymbol{e}_\theta|^2 \right] + \mathcal{E}(\boldsymbol{c}, \theta) \right)$$

$$= \min_{(\boldsymbol{c},\theta) \in \mathbb{R}^2 \times [-\pi,\pi]} \left(\min_{\boldsymbol{m} \in \mathbb{S}^1} \left[-\boldsymbol{h}_a \cdot \boldsymbol{m} + \frac{\kappa_{\mathrm{an}}^2}{2} |\boldsymbol{m} \times \boldsymbol{e}_\theta|^2 \right] + \mathcal{E}(\boldsymbol{c}, \theta) \right). \qquad (50)$$

The last equality (50), which reduces a minimization problem on $\mathbb{S}^2$ to a minimization problem on $\mathbb{S}^1$, is justified by the following argument. First, we observe that by using $\boldsymbol{m} = \pm \boldsymbol{e}_\theta$ as competitors, one can deduce the bound

$$\min_{\boldsymbol{m} \in \mathbb{S}^2} \left[-\boldsymbol{h}_a \cdot \boldsymbol{m} + \frac{\kappa_{\mathrm{an}}^2}{2} |\boldsymbol{m} \times \boldsymbol{e}_\theta|^2 \right] \leqslant -|\boldsymbol{h}_a \cdot \boldsymbol{e}_\theta| \leqslant 0. \qquad (51)$$

Thus, the minimization problem in (51) is solved by configuration with nonpositive energy. After that, we can exclude that $\boldsymbol{m} = \pm \boldsymbol{e}_3$ are minimizers of (51) given that the resulting energy would be strictly positive because of

$$-\boldsymbol{h}_a \cdot \boldsymbol{m} + \frac{\kappa_{\mathrm{an}}^2}{2} |\boldsymbol{m} \times \boldsymbol{e}_\theta|^2 = \frac{\kappa_{\mathrm{an}}^2}{2}.$$

Also, note that any minimizer of (51) has to be such that $\boldsymbol{h}_a \cdot \boldsymbol{m} = \boldsymbol{h}_a \cdot \boldsymbol{m}^\perp \geqslant 0$; otherwise, again, the energy would be strictly positive. That said, if $\boldsymbol{m} \cdot \boldsymbol{e}_3 \neq 0$, $\boldsymbol{m} \neq \pm \boldsymbol{e}_3$, and $\boldsymbol{h}_a \cdot \boldsymbol{m}^\perp \geqslant 0$ then

$$-\boldsymbol{h}_a \cdot \boldsymbol{m} + \frac{\kappa_{\mathrm{an}}^2}{2} |\boldsymbol{m} \times \boldsymbol{e}_\theta|^2 = \frac{\kappa_{\mathrm{an}}^2}{2} - |\boldsymbol{h}_a \cdot \boldsymbol{m}^\perp| - \frac{\kappa_{\mathrm{an}}^2}{2} (\boldsymbol{m}^\perp \cdot \boldsymbol{e}_\theta)^2$$

$$\geqslant \frac{\kappa_{\mathrm{an}}^2}{2} - \left| \boldsymbol{h}_a \cdot \frac{\boldsymbol{m}^\perp}{|\boldsymbol{m}^\perp|} \right| - \frac{\kappa_{\mathrm{an}}^2}{2} \left(\frac{\boldsymbol{m}^\perp}{|\boldsymbol{m}^\perp|} \cdot \boldsymbol{e}_\theta \right)^2$$

$$= -\boldsymbol{h}_a \cdot \frac{\boldsymbol{m}^\perp}{|\boldsymbol{m}^\perp|} + \frac{\kappa_{\mathrm{an}}^2}{2} \left| \frac{\boldsymbol{m}^\perp}{|\boldsymbol{m}^\perp|} \times \boldsymbol{e}_\theta \right|^2,$$

from which it follows that $\boldsymbol{m} = \frac{\boldsymbol{m}^\perp}{|\boldsymbol{m}^\perp|}$ has a lower energy density. Overall, we get that $\mathbb{S}^2$-minimizers of $\frac{\kappa_{\mathrm{an}}^2}{2} |\boldsymbol{m} \times \boldsymbol{e}_\theta|^2 - \boldsymbol{h}_a \cdot \boldsymbol{m}$ are actually elements of $\mathbb{S}^1$.

Remark 4.6. The vanishing of $\nabla \boldsymbol{m}$ in (35) is *not* an a priori hypothesis but follows from energy minimization. Roughly, as just shown in Step 1, the exchange term $a_{\mathrm{ex}}^2 \int_{\Omega_{\boldsymbol{c},\theta}} |\nabla \boldsymbol{m}|^2$ is strictly positive for any nonconstant magnetization, while the remaining terms can always be optimized within the class of spatially constant (in-plane) magnetizations. Hence, any nonconstant $\boldsymbol{m}$ incurs an uncompensated exchange penalty, and global minimizers have $\nabla \boldsymbol{m} = 0$, i.e., are single-domain.

Step 2. Solution of the minimization problem in the full controllability setting. From the previous step and Theorem 1, we get that if $L_0 \geqslant L + 2a$ then, as a function of $\boldsymbol{m} \in \mathbb{S}^1$, the energy density $(\kappa_{\mathrm{an}}^2/2) |\boldsymbol{m} \times \boldsymbol{e}_\theta|^2 - \boldsymbol{h}_a \cdot \boldsymbol{m}$ is minimized when θ is such that $\boldsymbol{e}_\theta = \pm \boldsymbol{h}_a / |\boldsymbol{h}_a|$, and $\boldsymbol{m} = \boldsymbol{h}_a / |\boldsymbol{h}_a|$ because in this case, we have

$$\frac{\kappa_{\mathrm{an}}^2}{2} |\boldsymbol{m} \times \boldsymbol{e}_\theta|^2 - \boldsymbol{h}_a \cdot \boldsymbol{m} = -|\boldsymbol{h}_a|.$$

After that, we recall that in the full controllability regime, the elastic energy has a minimizer $\Omega_{\boldsymbol{c},\theta}$ for every $\theta \in [\pi, \pi]$. It is sufficient to take $\boldsymbol{c} = \gamma_\delta(\theta)$. This implies that the minimal magnetoelastic energy is reached in the state $(\boldsymbol{m}; \boldsymbol{c}, \theta)$ with

$$\boldsymbol{m} = \frac{\boldsymbol{h}_a}{|\boldsymbol{h}_a|}, \quad R_\theta e_1 = \pm \frac{\boldsymbol{h}_a}{|\boldsymbol{h}_a|}, \quad \boldsymbol{c} = \gamma_\delta(\theta). \tag{52}$$

Indeed, for every $\boldsymbol{m} \in \mathbb{S}^1$, the following energy lower bound holds

$$\mathcal{G}(\boldsymbol{m}; \boldsymbol{c}, \theta) \geqslant -|\boldsymbol{h}_a|,$$

and with the choices in (52) we reach the equality $\mathcal{G}(\boldsymbol{m}; \boldsymbol{c}, \theta) = -|\boldsymbol{h}_a|$. This is the reason why we refer to the case $L_0 \geqslant L + 2a$ as the full controllability regime.

Instead, if $L < L_0 < L + 2a$, then, depending on the direction of the applied field $\boldsymbol{h}_a$, we have to distinguish between two possible scenarios. First, recall from (18) that the elastic energy vanishes whenever

$$\theta \in [-\cos^{-1}(1 - \delta), \cos^{-1}(1 - \delta)], \quad \delta := \frac{L_0^2 - L^2}{2a(a + L)}.$$

Given $\boldsymbol{h}_a \neq 0$, we denote by $\psi \in [-\pi, \pi]$ the angle that the applied field $\boldsymbol{h}_a$ makes with $\boldsymbol{e}_1$. If $\boldsymbol{h}_a / |\boldsymbol{h}_a| = R_\psi e_1$ for some $\psi \in [-\cos^{-1}(1 - \delta), \cos^{-1}(1 - \delta)]$, then the magnetoelastic minimizer is given by $(\boldsymbol{m}; \boldsymbol{c}, \theta)$ with $\boldsymbol{m} = \boldsymbol{h}_a / |\boldsymbol{h}_a|$, θ such that $\boldsymbol{e}_\theta = R_\theta e_1 = \pm \boldsymbol{h}_a / |\boldsymbol{h}_a|$ (i.e., $\theta = \psi + k\pi$, $k \in \mathbb{Z}$), and $\boldsymbol{c} = \gamma_\delta(\theta)$. Indeed, arguing as before, in this configuration, we have that $\boldsymbol{m} \times \boldsymbol{e}_\theta = 0$ and, therefore,

$$\mathcal{G}(\boldsymbol{m}; \boldsymbol{c}, \theta) = \mathcal{F}_{\Omega_{\boldsymbol{c},\theta}}(\boldsymbol{m}; \theta) = -|\boldsymbol{h}_a|.$$

It remains to understand the minimal configuration when $\boldsymbol{h}_a / |\boldsymbol{h}_a| = R_\psi e_1$ and $|\psi| > \cos^{-1}(1 - \delta)$. For that, we need to investigate the whole energy functional, which, thanks to Step 1 can be written as (cf. (49))

$$\mathcal{F}(\boldsymbol{m}; \boldsymbol{c}, \theta) := -\boldsymbol{h}_a \cdot \boldsymbol{m} + \frac{\kappa_{\mathrm{an}}^2}{2} |\boldsymbol{m} \times \boldsymbol{e}_\theta|^2 + \mathcal{E}(\boldsymbol{c}, \theta), \tag{53}$$

with

$$\mathcal{E}(\boldsymbol{c}, \theta) = \frac{1}{2} (|\boldsymbol{c} - \boldsymbol{v}_{a,L}(\theta)| - L_0)^2 + \frac{1}{2} (|\boldsymbol{c} + \boldsymbol{v}_{a,L}(\theta)| - L_0)^2. \tag{54}$$

Note that the minimization problem for $\mathcal{F}$ is finite-dimensional. However, given the nonconvex constraint $\boldsymbol{m} \in \mathbb{S}^1$, the critical points are solutions of a high order equation in the powers of $\boldsymbol{m} \cdot \boldsymbol{e}_\theta$ and $\boldsymbol{m} \cdot \boldsymbol{h}_a$. To proceed, it is convenient to express the quantities in polar coordinates through the angles (ϕ, ψ) whose meaning is given by

$$\boldsymbol{m} := R_\phi e_1, \quad \boldsymbol{h}_a := |\boldsymbol{h}_a| R_\psi e_1. \tag{55}$$

In this way, we have

$$\boldsymbol{h}_a \cdot \boldsymbol{m} = |\boldsymbol{h}_a| \, R_\psi \boldsymbol{e}_1 \cdot R_\phi \boldsymbol{e}_1 = |\boldsymbol{h}_a| \cos(\psi - \phi). \tag{56}$$

Similarly, we have

$$|\boldsymbol{m} \times \boldsymbol{e}_\theta|^2 = |\boldsymbol{m} \times R_\theta \boldsymbol{e}_1|^2 = 1 - \left(\boldsymbol{e}_1 \cdot R_\theta^\top R_\phi \boldsymbol{e}_1\right)^2 = \sin^2(\theta - \phi).$$

Therefore, the total magnetoelastic energy (38) reads as

$$\mathcal{F}(\boldsymbol{m}; \boldsymbol{c}, \theta) = \frac{\kappa_{\mathrm{an}}^2}{2} \sin^2(\theta - \phi) - |\boldsymbol{h}_a| \cos(\psi - \phi) + \mathcal{E}(\boldsymbol{c}, \theta) \tag{57}$$

The energy functional $\mathcal{F}$ has to be minimized in the configuration space $(\boldsymbol{c}, \theta, \phi) \in \mathbb{R}_+^2 \times [-\pi, \pi]^3$.

Step 3. Proof of (38). According to Proposition 1, depending on the strength of the physical parameters κ^2 and $|\boldsymbol{h}_a|$, the minimal angle θ can differ from the direction of the applied field (encoded in the angle ψ) and, in general, only numerical simulations can predict the behavior of the minimal magneto-elastic states. However, we can still predict the position of the center $\boldsymbol{c}$ depending on the minimal angle θ. For that, we observe that if $(\boldsymbol{c}, \theta)$ is a critical point of the elastic energy $\mathcal{E}$, then $\partial_{\boldsymbol{c}} \mathcal{E}(\boldsymbol{c}, \theta) = 0$. In expanded form, the stationary condition $\partial_{\boldsymbol{c}} \mathcal{E}(\boldsymbol{c}, \theta) = 0$ reads as

$$\partial_{\boldsymbol{c}} \mathcal{E}(\boldsymbol{c}, \theta) = (|\boldsymbol{c} + \boldsymbol{v}_{a,L}(\theta)| - L_0) \frac{\boldsymbol{c} + \boldsymbol{v}_{a,L}(\theta)}{|\boldsymbol{c} + \boldsymbol{v}_{a,L}(\theta)|}$$
$$+ (|\boldsymbol{c} - \boldsymbol{v}_{a,L}(\theta)| - L_0) \frac{\boldsymbol{c} - \boldsymbol{v}_{a,L}(\theta)}{|\boldsymbol{c} - \boldsymbol{v}_{a,L}(\theta)|} = 0. \tag{58}$$

In writing the previous relation, we assumed that $|\boldsymbol{c} + \boldsymbol{v}_{a,L}(\theta)| \neq 0$ and $|\boldsymbol{c} - \boldsymbol{v}_{a,L}(\theta)| \neq 0$. But actually, this is always the case for minimizers. To see this, we observe that if $|\boldsymbol{c} + \boldsymbol{v}_{a,L}(\theta)| = 0$ or $|\boldsymbol{c} - \boldsymbol{v}_{a,L}(\theta)| = 0$, then one of the two springs is at the maximal compression. Suppose that $|\boldsymbol{c} - \boldsymbol{v}_{a,L}(\theta)| = 0$, then $\boldsymbol{c} = \boldsymbol{v}_{a,L}(\theta)$ and the value of the associated elastic energy is

$$\mathcal{E}(\boldsymbol{v}_{a,L}(\theta), \theta) = \frac{1}{2} L_0^2 + \frac{1}{2} (2 |\boldsymbol{v}_{a,L}(\theta)| - L_0)^2.$$

On the other hand, $\boldsymbol{c} = 0$ has lower energy regardless of the angle θ. Indeed, we have

$$\mathcal{E}(\boldsymbol{v}_{a,L}(\theta), \theta) - \mathcal{E}(0, \theta) = \frac{1}{2} L_0^2 + \frac{1}{2} (2 |\boldsymbol{v}_{a,L}(\theta)| - L_0)^2 - (|\boldsymbol{v}_{a,L}(\theta)| - L_0)^2$$
$$= \frac{1}{2} L_0^2 + \frac{1}{2} \left(4 |\boldsymbol{v}_{a,L}(\theta)|^2 + L_0^2 - 4L_0 |\boldsymbol{v}_{a,L}(\theta)|\right)$$
$$- \left(|\boldsymbol{v}_{a,L}(\theta)|^2 + L_0^2 - 2L_0 |\boldsymbol{v}_{a,L}(\theta)|\right)$$
$$= \frac{1}{2} L_0^2 + 2 |\boldsymbol{v}_{a,L}(\theta)|^2 + \frac{1}{2} L_0^2 - 2L_0 |\boldsymbol{v}_{a,L}(\theta)|$$
$$- |\boldsymbol{v}_{a,L}(\theta)|^2 - L_0^2 + 2L_0 |\boldsymbol{v}_{a,L}(\theta)|$$
$$= |\boldsymbol{v}_{a,L}(\theta)|^2,$$

and we know from (16) that $|\boldsymbol{v}_{a,L}(\theta)|^2 \geqslant L^2$. This means that the choice $\boldsymbol{c} = \boldsymbol{v}_{a,L}(\theta)$ never gives an energy-minimizing configuration. The same argument applies to the

$|\boldsymbol{c} + \boldsymbol{v}_{a,L}(\theta)| = 0$. Overall, we have shown that if $(\boldsymbol{c}, \theta)$ is a minimum point of the elastic energy $\mathcal{E}$ then $|\boldsymbol{c} \pm \boldsymbol{v}_{a,L}(\theta)| \neq 0$, i.e.,

$$\boldsymbol{c} \neq \pm \boldsymbol{v}_{a,L}(\theta). \tag{59}$$

As a side remark, note that this observation holds regardless of the current regime $L < L_0 < L + 2a$.

Having proved that (58) is well-defined at minima, we observe that (58) implies, in particular, that at minima *equipartition of the energy* holds:

$$\frac{1}{2} \left(|\boldsymbol{c} - \boldsymbol{v}_{a,L}(\theta)| - L_0\right)^2 = \frac{1}{2} \left(|\boldsymbol{c} + \boldsymbol{v}_{a,L}(\theta)| - L_0\right)^2. \tag{60}$$

In other words, at equilibrium, the variation in absolute value of the length of the two springs (computed with respect to the rest length L_0) is the same for the two springs.

The previous relation allows us to focus on the case $|\boldsymbol{c} \pm \boldsymbol{v}_{a,L}(\theta)| - L_0 \neq 0$. Indeed, if θ is such that $|\boldsymbol{c} \pm \boldsymbol{v}_{a,L}(\theta)| = L_0$, then we already know from Theorem 1 that minimizers have zero elastic energy, the angle θ is such that

$$\cos\theta \geqslant 1 - \delta \quad \text{with} \quad \delta := \frac{L_0^2 - L^2}{2a(a+L)}, \tag{61}$$

and the position of $\boldsymbol{c}$ is given by (20) and (21).

From (58) and (60) we get that if $|\boldsymbol{c} \pm \boldsymbol{v}_{a,L}(\theta)| - L_0 \neq 0$, then

$$\frac{\boldsymbol{c} + \boldsymbol{v}_{a,L}(\theta)}{|\boldsymbol{c} + \boldsymbol{v}_{a,L}(\theta)|} = \pm \frac{\boldsymbol{c} - \boldsymbol{v}_{a,L}(\theta)}{|\boldsymbol{c} - \boldsymbol{v}_{a,L}(\theta)|}. \tag{62}$$

In particular, the wedge product of $\boldsymbol{c} + \boldsymbol{v}_{a,L}(\theta)$ with $\boldsymbol{c} - \boldsymbol{v}_{a,L}(\theta)$ vanishes, i.e.,

$$(\boldsymbol{c} + \boldsymbol{v}_{a,L}(\theta)) \times (\boldsymbol{c} - \boldsymbol{v}_{a,L}(\theta)) = 0. \tag{63}$$

The previous expression simplifies to

$$\boldsymbol{c} \times \boldsymbol{v}_{a,L}(\theta) = 0. \tag{64}$$

The previous relation (64) implies that if $(\boldsymbol{c}, \theta)$ is a stationary point for $\mathcal{E}$ (satisfying (59)) then $\boldsymbol{c} = \lambda \boldsymbol{v}_{a,L}(\theta)$ for some $\lambda \in \mathbb{R}$ with $\lambda \neq \pm 1$.

However, a direct computation shows that either $\lambda = 0$ or $\lambda = \frac{L_0}{|\boldsymbol{v}_{a,L}(\theta)|}$. Indeed, for $\boldsymbol{c} = \lambda \boldsymbol{v}_{a,L}(\theta)$ we have

$$\partial_{\boldsymbol{c}} \mathcal{E}(\boldsymbol{c}, \theta) = (|1 + \lambda| \cdot |\boldsymbol{v}_{a,L}(\theta)| - L_0) \cdot \text{sgn}(1 + \lambda) \frac{\boldsymbol{v}_{a,L}(\theta)}{|\boldsymbol{v}_{a,L}(\theta)|}$$
$$- (|1 - \lambda| \cdot |\boldsymbol{v}_{a,L}(\theta)| - L_0) \, \text{sgn}(1 - \lambda) \frac{\boldsymbol{v}_{a,L}(\theta)}{|\boldsymbol{v}_{a,L}(\theta)|}. \tag{65}$$

Therefore, if $|\lambda| < 1$ then

$$
\begin{aligned}
\partial_{\boldsymbol{c}}\mathcal{E}(\boldsymbol{c}, \theta) &= ((1+\lambda) \cdot |\boldsymbol{v}_{a,L}(\theta)| - L_0) \frac{\boldsymbol{v}_{a,L}(\theta)}{|\boldsymbol{v}_{a,L}(\theta)|} \\
&\qquad - ((1-\lambda) \cdot |\boldsymbol{v}_{a,L}(\theta)| - L_0) \frac{\boldsymbol{v}_{a,L}(\theta)}{|\boldsymbol{v}_{a,L}(\theta)|} \\
&= 2\lambda \, |\boldsymbol{v}_{a,L}(\theta)|
\end{aligned}
\tag{66}
$$

and the right-hand side vanishes if, and only if, $\lambda = 0$. On the other hand, if $\lambda > 1$ then

$$
\begin{aligned}
\partial_{\boldsymbol{c}}\mathcal{E}(\boldsymbol{c}, \theta) &= ((1+\lambda) \cdot |\boldsymbol{v}_{a,L}(\theta)| - L_0) \frac{\boldsymbol{v}_{a,L}(\theta)}{|\boldsymbol{v}_{a,L}(\theta)|} \\
&\qquad + ((\lambda-1) \cdot |\boldsymbol{v}_{a,L}(\theta)| - L_0) \frac{\boldsymbol{v}_{a,L}(\theta)}{|\boldsymbol{v}_{a,L}(\theta)|} \\
&= 2 \left(\lambda |\boldsymbol{v}_{a,L}(\theta)| - L_0\right) \frac{\boldsymbol{v}_{a,L}(\theta)}{|\boldsymbol{v}_{a,L}(\theta)|}
\end{aligned}
\tag{67}
$$

and the right-hand side vanishes if, and only if, $\lambda = \frac{L_0}{|\boldsymbol{v}_{a,L}(\theta)|}$. Similarly, if $\lambda < -1$ then

$$
\partial_{\boldsymbol{c}}\mathcal{E}(\boldsymbol{c}, \theta) = 2 \left(\lambda \cdot |\boldsymbol{v}_{a,L}(\theta)| + L_0\right) \frac{\boldsymbol{v}_{a,L}(\theta)}{|\boldsymbol{v}_{a,L}(\theta)|}
$$

and the right-hand side vanishes if, and only if, $\lambda = -L_0/|\boldsymbol{v}_{a,L}(\theta)|$.

Summarizing, in the regime $L < L_0 < L + 2a$ we have that if $(\boldsymbol{m}; \boldsymbol{c}, \theta)$ is a stationary point of the magnetoelastic energy, then the following alternatives are possible for the position of the center $\boldsymbol{c}$ (in what follows, as usual, $\delta := (L_0^2 - L^2)/(2a(a+L))$):

i.   There holds $\cos\theta \geqslant 1 - \delta$; in which case $\mathcal{E}(\boldsymbol{c}, \theta) = 0$ with the optimal center $\boldsymbol{c}$ determined by the curve γ_δ defined by (20) and (21).

ii. There holds $\cos\theta < 1 - \delta$ and $\lambda = 0$; in which case $\boldsymbol{c} = 0$.

iii. There holds $\cos\theta < 1 - \delta$ and $\lambda = \pm L_0/|\boldsymbol{v}_{a,L}(\theta)|$ with $L_0 > |\boldsymbol{v}_{a,L}(\theta)|$ and; in which case $\boldsymbol{c} = \pm L_0 \boldsymbol{v}_{a,L}(\theta)/|\boldsymbol{v}_{a,L}(\theta)|$ (and $|\boldsymbol{c}| = L_0$).

From the previous possibilities, it appears clear that a full characterization of the minimal center $\boldsymbol{c}$ associated with θ is achieved as soon as we compare the energy associated with possibilities *ii* and *iii*. For that, recalling that $|\lambda| > 1$, we have

$$
\begin{aligned}
\mathcal{E}\left(\lambda\boldsymbol{v}_{a,L}(\theta), \theta\right) &= \left(|\lambda - 1| \, |\boldsymbol{v}_{a,L}(\theta)| - L_0\right)^2 \\
&= \left(\left|\pm\frac{L_0}{|\boldsymbol{v}_{a,L}(\theta)|} - 1\right| \, |\boldsymbol{v}_{a,L}(\theta)| - L_0\right)^2 \\
&= \left(|\pm L_0 - |\boldsymbol{v}_{a,L}(\theta)|| - L_0\right)^2 \\
&= |\boldsymbol{v}_{a,L}(\theta)|^2 \,.
\end{aligned}
$$

Also, we have

$$
\mathcal{E}(0, \theta) = \qquad \left(|\boldsymbol{v}_{a,L}(\theta)| - L_0\right)^2 = |\boldsymbol{v}_{a,L}(\theta)|^2 - 2L_0 \, |\boldsymbol{v}_{a,L}(\theta)| + L_0^2.
$$

Hence, when $\cos\theta < 1 - \delta$, the center $\boldsymbol{c} = 0$ is energetically favored whenever $|\boldsymbol{v}_{a,L}(\theta)| > L_0/2$. From the expression of $|\boldsymbol{v}_{a,L}(\theta)|$ we get that this happens if, and only if,

$$a^2 \sin^2\theta + (a(1 - \cos\theta) + L)^2 > L_0^2/4.$$

Simplifying the previous expression, we see that this happens when

$$\cos(\theta) < \frac{2a^2 + 2aL + L^2 - L_0^2/4}{2a(a+L)} = \frac{2a(a+L) + L^2 - L_0^2/4}{2a(a+L)} = 1 - \frac{L_0^2/4 - L^2}{2a(a+L)}.$$

But this is always the case because by assumption $\cos\theta < 1 - \delta$ and, on the other hand,

$$1 - \delta < 1 - \frac{L_0^2/4 - L^2}{2a(a+L)}.$$

This concludes the proof. $\qquad\square$

5. Conclusion

We introduced a minimal variational model for a rigid, permanently magnetized ellipse tethered by two linear springs and driven by a homogeneous in-plane field, and proved two sharp structural results: Theorem 1 characterizes the continuous family of zero-energy elastic equilibria, and Theorem 2 identifies the *full-controllability* regime $L_0 \geqslant L + 2a$ in which the particle's center and orientation follow the applied field without elastic penalty.

These findings give immediate, practical design rules: choose the rest length to satisfy $L_0 \geqslant L + 2a$ for maximal, low-energy manoeuvrability; outside that regime, elastic pinning and multistability appear and can be exploited for switchable or bistable devices. Our reduction to a single-domain micromagnetic model clarifies how magnetic strength and anisotropy compete with elasticity (spring stiffness enters as a simple rescaling of the effective magnetic parameters), which is useful for engineering tradeoffs.

These findings yield simple, quantitative design rules for magnetoelastic microactuators and metamaterial building blocks and suggest direct applications in wireless microrobotics, MEMS, reconfigurable surfaces, and biomedical microdevices where low-energy, remotely controlled orientation and positioning are desirable.

Finally, the work points to several natural follow-ups: (i) a systematic mapping of the $(|\boldsymbol{h}_a|, \kappa_{\mathrm{an}}, L_0, L, a)$ parameter space, (ii) a detailed study of the nonconvex Stoner–Wohlfarth–elastic energy $\mathcal{F}$ for switching and hysteresis (see (39)), and (iii) extensions that incorporate spring bending/buckling and dynamical effects for time-dependent actuation.

Overall, the results provide compact, actionable criteria for planar control of tethered magnetic particles and point to several attainable experimental and theoretical next steps.

Author Contributions. G. Di Fratta, C. Serpico, and V. Slastikov contributed equally to all the results of this article.

Data Availability. Data sharing does not apply to this article as no datasets were generated or analyzed during this study.

Conflict of Interest. The authors declare no conflict of interest.

References

[1] C. A. Brisbois and M. O. de la Cruz, *Locomotion of magnetoelastic membranes in viscous fluids*, Physical Review Research, 4 (2022), p. 023166.

[2] C. A. Brisbois, M. Tasinkevych, P. Vázquez-Montejo, and M. Olvera de la Cruz, *Actuation of magnetoelastic membranes in precessing magnetic fields*, Proceedings of the National Academy of Sciences, 116 (2019), pp. 2500–2505.

[3] W. F. Brown, *Micromagnetics*, Interscience Publishers, 1963.

[4] J. M. Dempster, P. Vázquez-Montejo, and M. Olvera de la Cruz, *Contractile actuation and dynamical gel assembly of paramagnetic filaments in fast precessing fields*, Physical Review E, 95 (2017), p. 052606.

[5] A. DeSimone and G. Dolzmann, *Existence of minimizers for a variational problem in two-dimensional nonlinear magnetoelasticity*, Archive for Rational Mechanics and Analysis, 144 (1998), pp. 107–120.

[6] A. DeSimone and R. D. James, *A constrained theory of magnetoelasticity*, Journal of the Mechanics and Physics of Solids, 50 (2002), pp. 283–320.

[7] G. Di Fratta, C. B. Muratov, F. N. Rybakov, and V. V. Slastikov, *Variational principles of micromagnetics revisited*, SIAM Journal on Mathematical Analysis, 52 (2020), pp. 3580–3599.

[8] G. Di Fratta, *Micromagnetics of curved thin films*, Zeitschrift für angewandte Mathematik und Physik, 71 (2020).

[9] L. Dorfmann and R. W. Ogden, *Nonlinear Theory of Electroelastic and Magnetoelastic Interactions*, vol. 112, Springer US, 2014.

[10] R. Dreyfus, J. Baudry, M. L. Roper, M. Fermigier, H. A. Stone, and J. Bibette, *Microscopic artificial swimmers*, Nature, 437 (2005), pp. 862–865.

[11] G. Gioia and R. D. James, *Micromagnetics of very thin films*, Proceedings of the Royal Society of London. Series A: Mathematical, Physical and Engineering Sciences, 453 (1997), pp. 213–223.

[12] C. S. Isaak D. Mayergoyz, Giorgio Bertotti, *Nonlinear Magnetization Dynamics in Nanosystems*, Elsevier, 2009.

[13] M. Lapine, I. V. Shadrivov, D. A. Powell, and Y. S. Kivshar, *Magnetoelastic metamaterials*, Nature Materials, 11 (2011), pp. 30–33.

[14] D. Liu, R. Guo, B. Wang, J. Hu, and Y. Lu, *Magnetic micro/nanorobots: A new age in biomedicines*, Advanced Intelligent Systems, 4 (2022), p. 2200208.

[15] D. Niarchos, *Magnetic mems: key issues and some applications*, Sensors and Actuators A: Physical, 106 (2003), pp. 255–262.

[16] M. Poty, F. Weyer, G. Grosjean, G. Lumay, and N. Vandewalle, *Magnetoelastic instability in soft thin films*, The European Physical Journal E, 40 (2017), p. 29.

[17] E. Stoner and E. Wohlfarth, *A mechanism of magnetic hysteresis in heterogeneous alloys*, Philosophical Transactions of the Royal Society of London. Series A, Mathematical and Physical Sciences, 240 (1948), pp. 599–642.

[18] R.-J. Yang, H.-H. Hou, Y.-N. Wang, and L.-M. Fu, *Micro-magnetofluidics in microfluidic systems: A review*, Sensors and Actuators B: Chemical, 224 (2016), pp. 1–15.

[19] Z. Yang and L. Zhang, *Magnetic actuation systems for miniature robots: A review*, Advanced Intelligent Systems, 2 (2020), p. 2000082.

[20] H. Zhou, C. C. Mayorga-Martinez, S. Pané, L. Zhang, and M. Pumera, *Magnetically driven micro and nanorobots*, Chemical Reviews, 121 (2021), pp. 4999–5041.

G. Di Fratta, Dipartimento di Matematica e Applicazioni "R. Caccioppoli", Università degli Studi di Napoli "Federico II", Via Cintia, Complesso Monte S. Angelo, 80126 Naples, Italy.

E-mail: giovanni.difratta@unina.it.

C. Serpico, Department of Electrical Engineering and ICT, Università degli Studi di Napoli "Federico II", Via Claudio, 80126 Naples, Italy.

E-mail: serpico@unina.it.

Valeriy Slastikov, School of Mathematics, University of Bristol, University Walk, Bristol BS8 1TW, United Kingdom.

E-mail: valeriy.slastikov@bristol.ac.uk.